

Experimental Evidence for a Triplet Biradical Excited-State Mechanism in the Photoreactivity of N,C-Chelate Organoboron Compounds

Supporting Information

Soren K. Mellerup^{\$}, Goonay Yousefalizadeh^{\$}, Suning Wang* and Kevin Stamplecoskie*

Department of Chemistry, Queen's University, Kingston, Ontario K7L3N6, Canada

* Suning.wang@chem.queensu.ca

* kevin.stamplecoskie@queensu.ca

Section S1. Steady-State Absorbance and Fluorescence Data of 1–3 in THF.

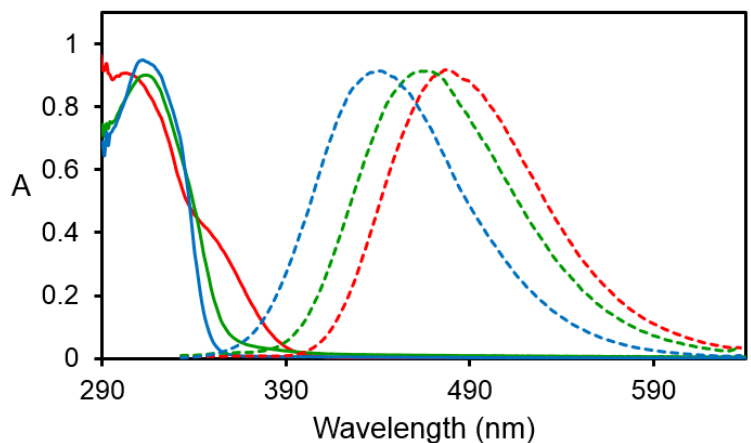


Figure S1. UV/vis (solid) and fluorescence (dashed) spectra of **1–3** in THF at 10^{-4} M.

Table S1. Summary of the steady-state photophysical properties for **1–3**.

	λ_{abs} , nm (ϵ ; $\text{M}^{-1} \text{cm}^{-1}$)	λ_{em} , nm	Φ_{em} (± 0.05)
1	312, 345(bs) (9075)	477	0.28
2	315 (9023)	468	0.20
3	315 (9518)	441	0.37

*bs = broad shoulder; Measured in THF at 10^{-4} M.

Section S2. Excited-State Dynamics of 1–3.

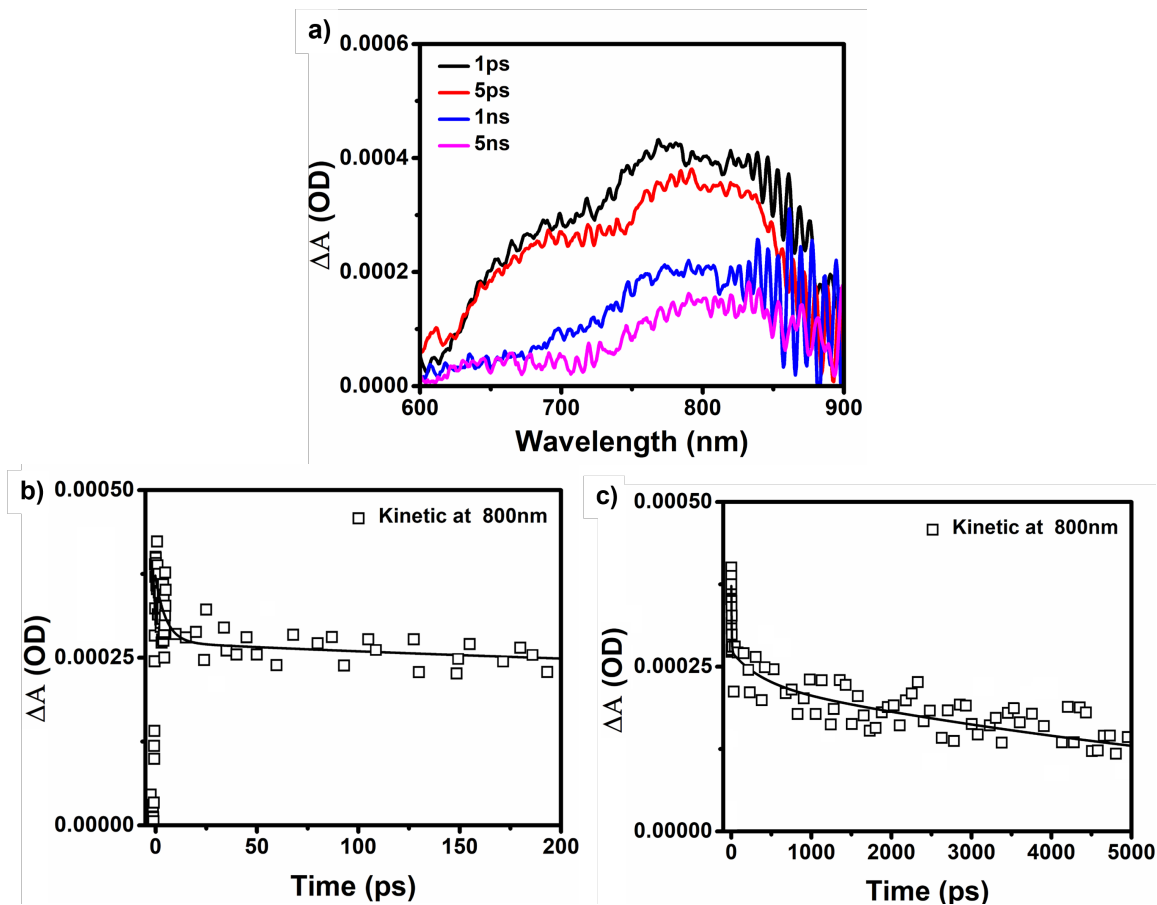


Figure S2. Femtosecond transient ΔA spectra of compound **1** at varying delay times ($t = 1, 5, 1000$, and 5000 ps) in THF (a), and decay traces with corresponding fits monitored at 800 nm over short (200 ps; b) and long (5 ns; c) time intervals.

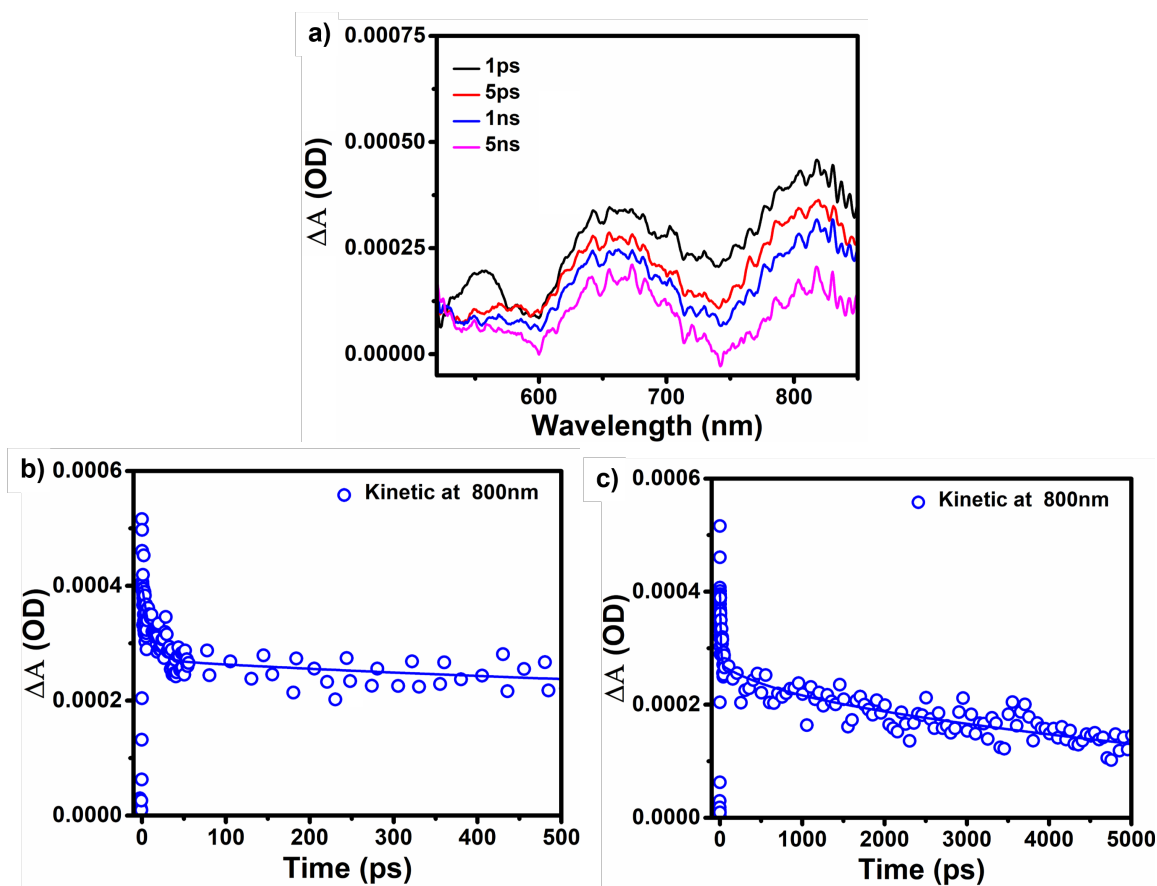


Figure S3. Femtosecond transient ΔA spectra of compound **2** at varying delay times ($t = 1, 5, 1000$, and 5000 ps) in THF (a), and decay traces with corresponding fits monitored at 800 nm over short (200 ps; b) and long (5 ns; c) time intervals.

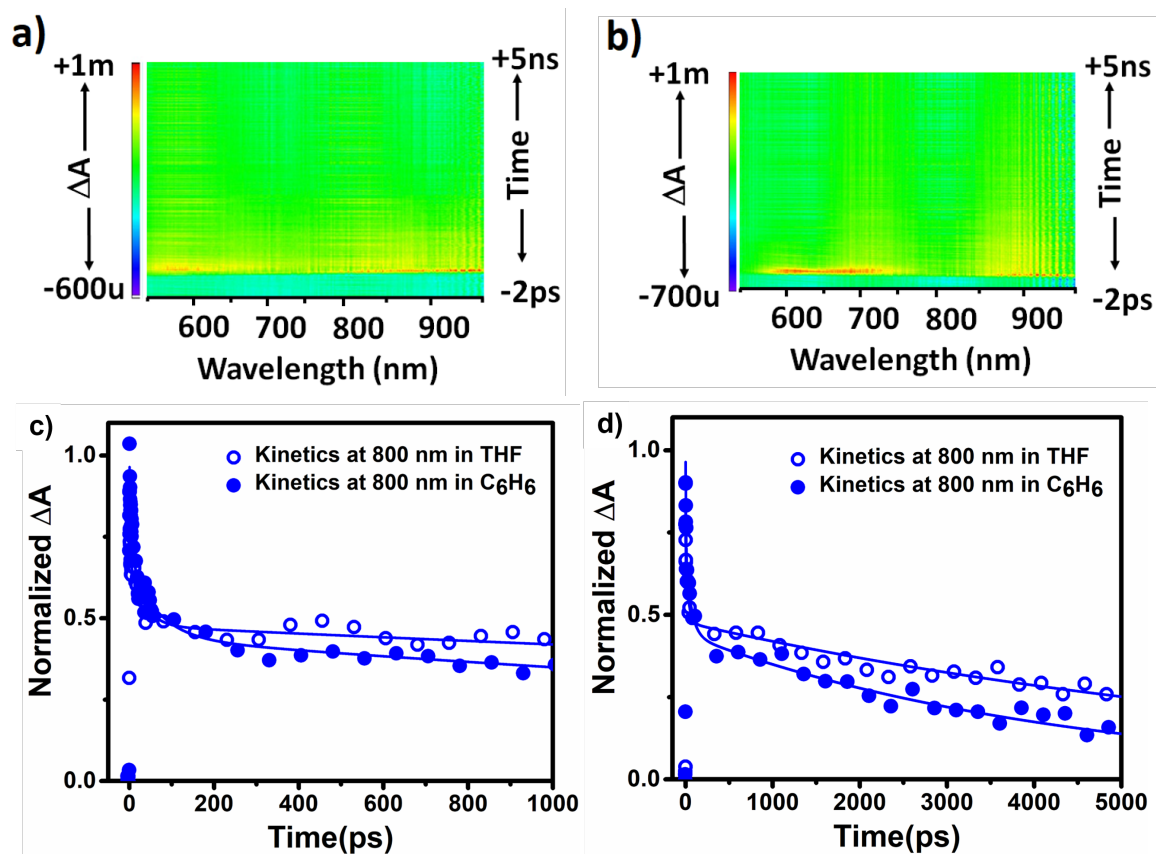


Figure S4. Femtosecond transient ΔA spectra of compound **2** up to 5 ns with 340 nm excitation in C_6H_6 (a) and THF (b), as well as the overlaid kinetic plots (c) at 800 nm over short (left) and long (right) time intervals.

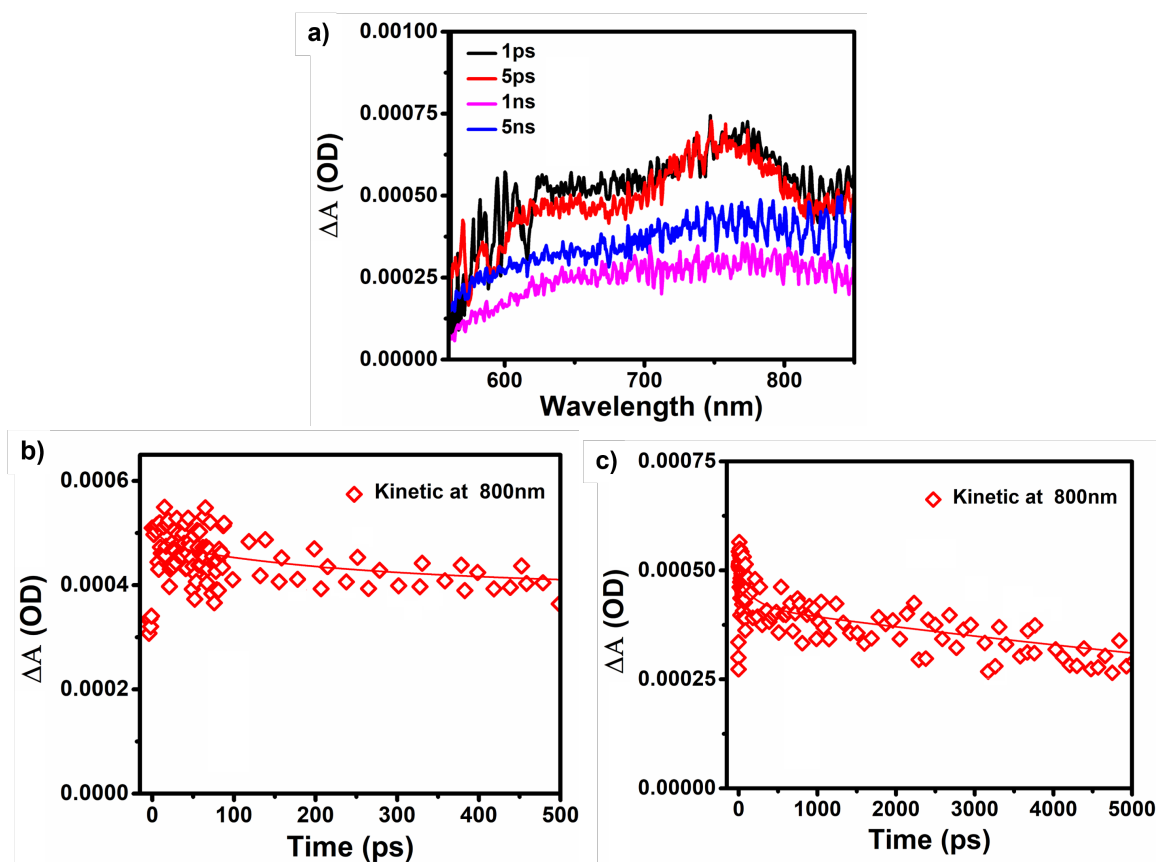


Figure S5. Femtosecond transient ΔA spectra of compound **3** at varying delay times ($t = 1, 5, 1000$, and 5000 ps) in THF (a), and decay traces with corresponding fits monitored at 800 nm over short (200 ps; b) and long (5 ns; c) time intervals.

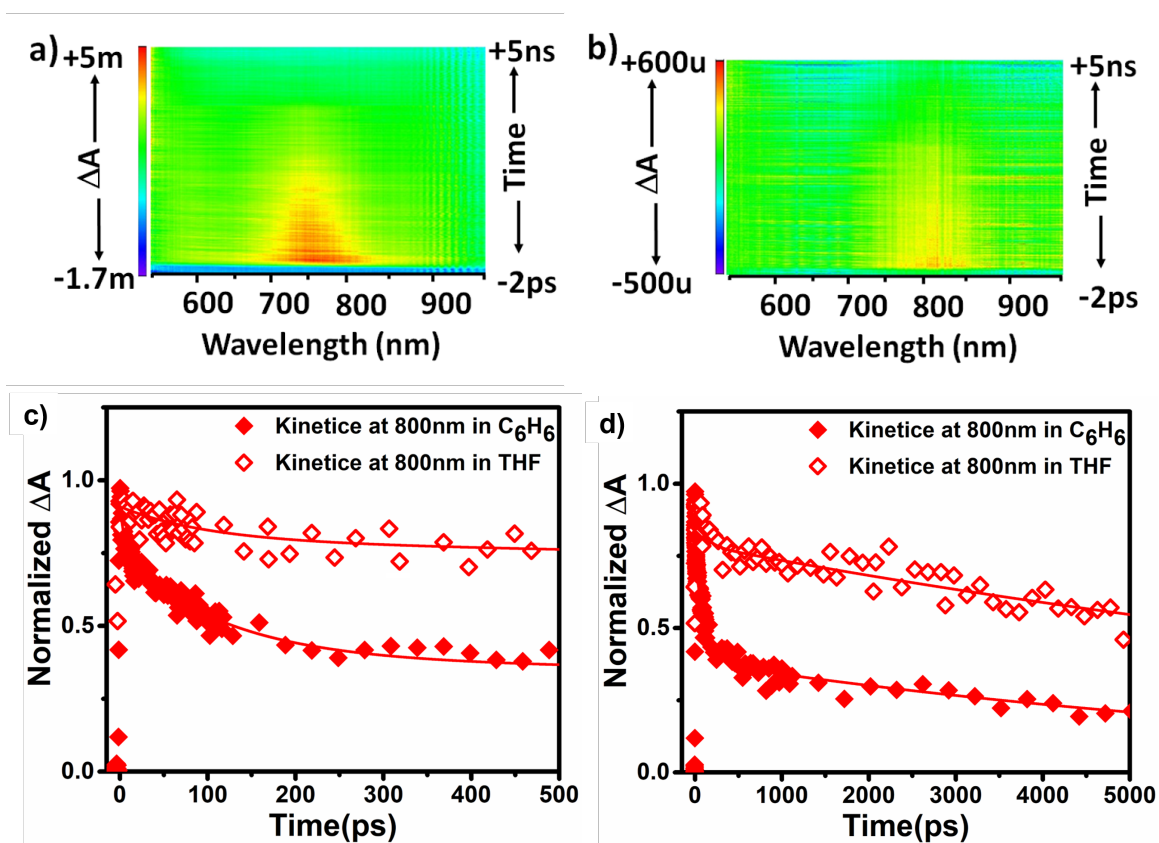
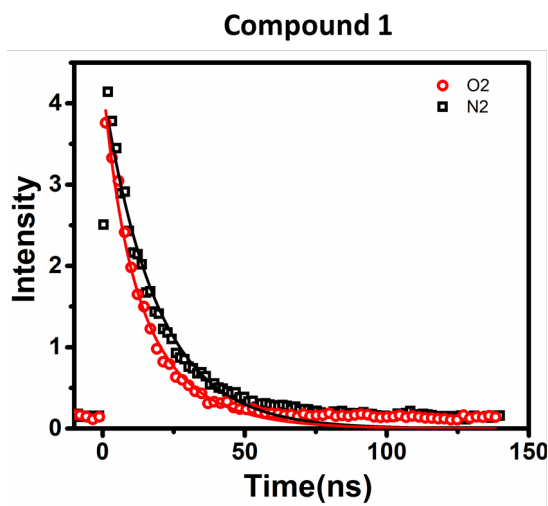


Figure S6. Femtosecond transient ΔA spectra of compound **3** up to 5 ns with 340 nm excitation in C_6H_6 (a) and THF (b), as well as the overlaid kinetic plots (c) at 800 nm over short (left) and long (right) time intervals.

Section S3. Long Lifetimes of 1–3.



$t_1(\text{ns})$	$t_2(\text{ns})$	$K_1(\text{ns}^{-1}\text{M})$	$K_2(\text{ns}^{-1}\text{M})$
18.82	7.03	0.052	0.142

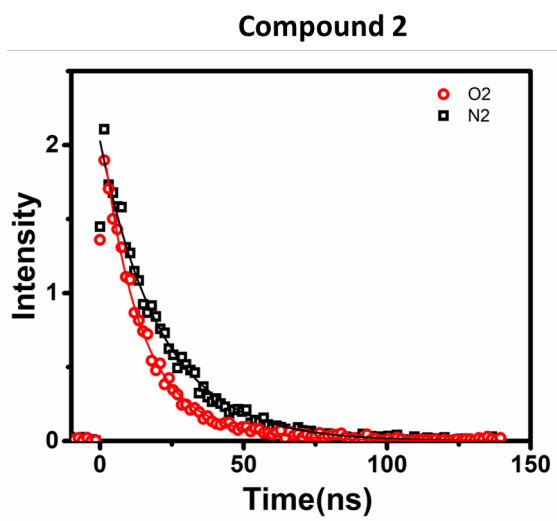
$$\tau_1 = \frac{1}{K_1} = \frac{1}{0.052} = 19.23 \text{ ns}$$

$$\langle \tau \rangle = \frac{A_1 \tau_1^2 + A_2 \tau_2^2 + \dots}{A_1 \tau_1 + A_2 \tau_2 + \dots} = \frac{A_1 \tau_1^2}{A_1 \tau_1} = \frac{\tau_1^2}{\tau_1} = \tau_1 = 19.23 \text{ ns}$$

$$K_2 = K_Q[Q]$$

$$k_Q = \frac{0.142\text{E}9}{0.04} = 3.55\text{E}9 \text{ s}^{-1}\text{M}$$

Figure S7. Stead-state luminescence lifetimes of **1** measured in C_6H_6 under N_2 (black) and atmospheric conditions (red) at 10^{-4}M , as well as their calculated mono-exponential decays and K_Q .¹



$t_1(\text{ns})$	$t_2(\text{ns})$	$K_1(\text{ns}^{-1}\text{M})$	$K_2(\text{ns}^{-1}\text{M})$
21.14	11.13	0.047	0.089

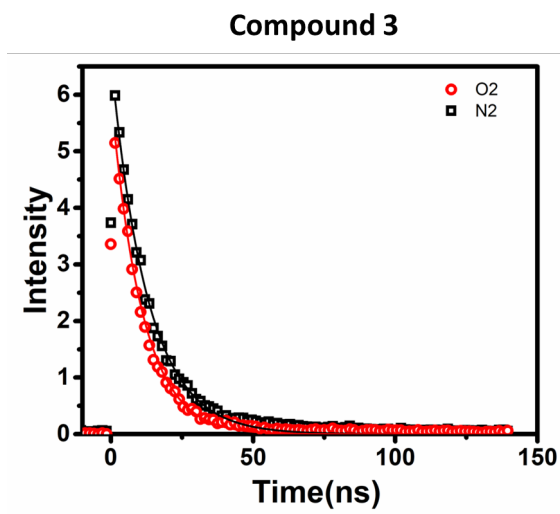
$$\tau_1 = \frac{1}{K_1} = \frac{1}{0.047} = 21.27 \text{ ns}$$

$$\langle \tau \rangle = \frac{A_1 \tau_1^2 + A_2 \tau_2^2 + \dots}{A_1 \tau_1 + A_2 \tau_2 + \dots} = \frac{A_1 \tau_1^2}{A_1 \tau_1} = \frac{\tau_1^2}{\tau_1} = \tau_1 = 21.27 \text{ ns}$$

$$K_2 = K_Q[Q]$$

$$k_Q = \frac{0.089\text{E}9}{0.04} = 2.24\text{E}9 \text{ s}^{-1}\text{M}$$

Figure S8. Stead-state luminescence lifetimes of **2** measured in C_6H_6 under N_2 (black) and atmospheric conditions (red) at 10^{-4}M , as well as their calculated mono-exponential decays and K_Q .¹



$\tau_1(\text{ns})$	$\tau_2(\text{ns})$	$K_1(\text{ns}^{-1}\text{M})$	$K_2(\text{ns}^{-1}\text{M})$
12.74	10.77	0.078	0.092

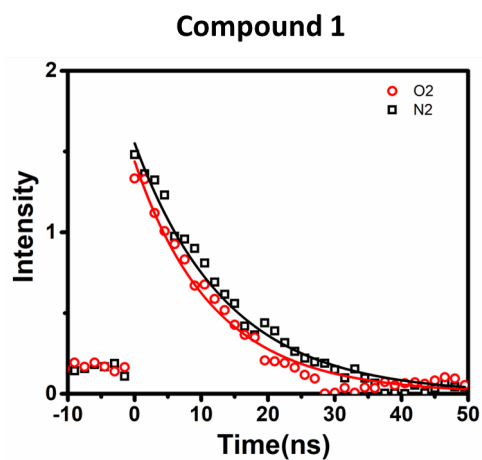
$$\tau_1 = \frac{1}{K_1} = \frac{1}{0.078} = 12.75 \text{ ns}$$

$$\langle \tau \rangle = \frac{A_1 \tau_1^2 + A_2 \tau_2^2 + \dots}{A_1 \tau_1 + A_2 \tau_2 + \dots} = \frac{A_1 \tau_1^2}{A_1 \tau_1} = \frac{\tau_1^2}{\tau_1} = \tau_1 = 12.75 \text{ ns}$$

$$K_2 = K_Q[Q]$$

$$k_Q = \frac{0.092 \text{E}9}{0.04} = 2.32 \text{E}9 \text{ s}^{-1}\text{M}$$

Figure S9. Stead-state luminescence lifetimes of **3** measured in C_6H_6 under N_2 (black) and atmospheric conditions (red) at 10^{-4} M , as well as their calculated mono-exponential decays and K_Q .¹



$t_1(\text{ns})$	$t_2(\text{ns})$	$K_1(\text{ns}^{-1}\text{M})$	$K_2(\text{ns}^{-1}\text{M})$
13.72	9.26	0.072	0.107

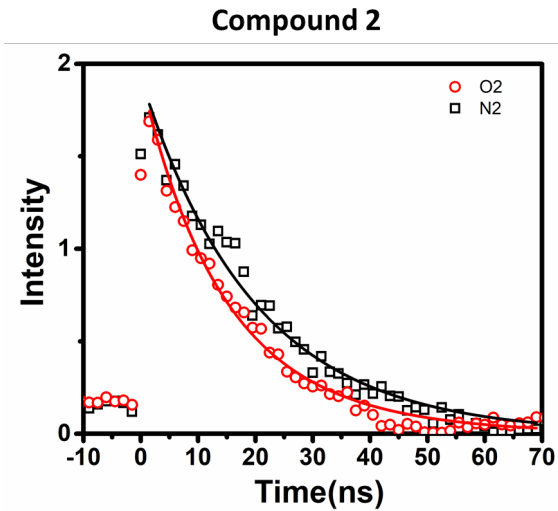
$$\tau_1 = \frac{1}{K_1} = \frac{1}{0.072} = 13.73 \text{ ns}$$

$$\langle \tau \rangle = \frac{A_1 \tau_1^2 + A_2 \tau_2^2 + \dots}{A_1 \tau_1 + A_2 \tau_2 + \dots} = \frac{A_1 \tau_1^2}{A_1 \tau_1} = \frac{\tau_1^2}{\tau_1} = \tau_1 = 13.73 \text{ ns}$$

$$K_2 = K_Q[Q]$$

$$k_Q = \frac{0.107\text{E}9}{0.0418} = 2.56\text{E}9 \text{ s}^{-1}\text{M}$$

Figure S10. Stead-state luminescence lifetimes of **1** measured in THF under N₂ (black) and atmospheric conditions (red) at 10⁻⁴ M, as well as their calculated mono-exponential decays and K_Q.²



$t_1(\text{ns})$	$t_2(\text{ns})$	$K_1(\text{ns}^{-1}\text{M})$	$K_2(\text{ns}^{-1}\text{M})$
19.82	11.90	0.050	0.083

$$\tau_1 = \frac{1}{K_1} = \frac{1}{0.050} = 19.84 \text{ ns}$$

$$\langle \tau \rangle = \frac{A_1 \tau_1^2 + A_2 \tau_2^2 + \dots}{A_1 \tau_1 + A_2 \tau_2 + \dots} = \frac{A_1 \tau_1^2}{A_1 \tau_1} = \frac{\tau_1^2}{\tau_1} = \tau_1 = 19.84 \text{ ns}$$

$$K_2 = K_Q[Q]$$

$$k_Q = \frac{0.083\text{E}9}{0.0418} = 2.007\text{E}9 \text{ s}^{-1}\text{M}$$

Figure S11. Stead-state luminescence lifetimes of **2** measured in THF under N₂ (black) and atmospheric conditions (red) at 10⁻⁴ M, as well as their calculated mono-exponential decays and K_Q.²

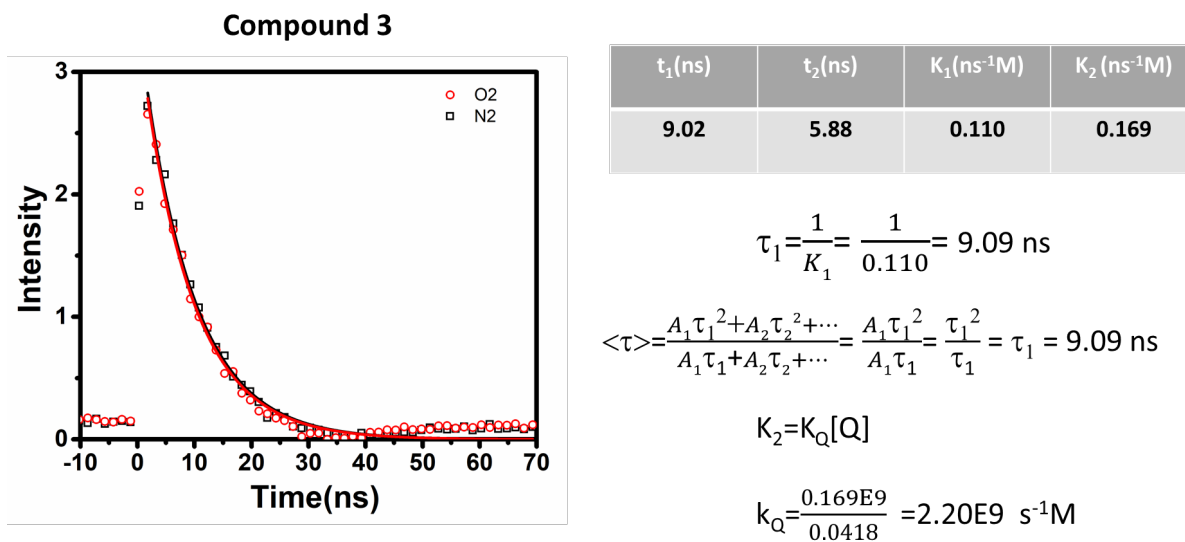


Figure S12. Stead-state luminescence lifetimes of **3** measured in THF under N₂ (black) and atmospheric conditions (red) at 10⁻⁴ M, as well as their calculated mono-exponential decays and K_Q.²

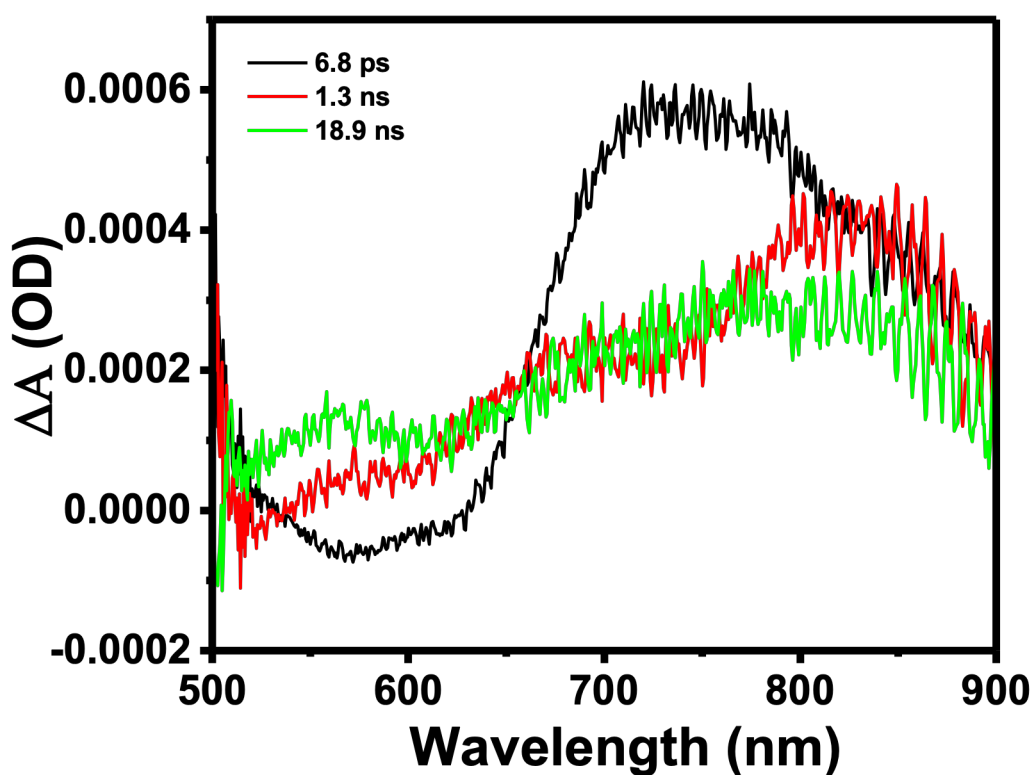


Figure S13. Global analysis of decay associated difference spectra for compound 1

Section S4. References.

- 1) Sato, T.; Hamada, Y.; Sumikawa, M.; Araki, S.; Yamamoto, H. Solubility of Oxygen in Organic Solvents and Calculation of the Hansen Solubility Parameters of Oxygen. *Ind. Eng. Chem. Res.* **2014**, *53*, 19331–19337.
- 2) Lawrence Clever, H.; Battino, R.; Miyamoto, H.; Yampolski, Y.; Young, C. L. IUPAC-NIST Solubility Data Series. 103. Oxygen and Ozone in Water, Aqueous Solutions, and Organic Liquids (Supplement to Solubility Data Series Volume 7). *J. Phys. Chem. Ref. Data* **2014**, *43*, 033102.